Simulation and analysis of secondary organic aerosol dynamics in the South Coast Air Basin of California

Satish Vutukuru, 1 Robert J. Griffin, 2 and Donald Dabdub 1

Received 27 April 2005; revised 16 August 2005; accepted 17 November 2005; published 26 May 2006.

[1] The dynamics of secondary organic aerosol (SOA) formation are analyzed using a species-resolved SOA model for the South Coast Air Basin of California (SoCAB). Updated versions of the Caltech Atmospheric Chemistry Mechanism (CACM) and the Model to Predict the Multiphase Partitioning of Organics (MPMPO) are integrated with the CIT airshed model. The simulations are performed using input data from the 8-9 September 1993 episode. Results show that urban areas with major volatile organic compound (VOC) emission sites experience peaks in SOA levels during morning hours. Downwind locations, such as Azusa and Claremont, experience sustained levels of high SOA concentrations in comparison with coastal areas such as central Los Angeles and Long Beach. Concentrations of condensible organics are higher in inland locations compared to those in coastal locations because of high oxidation capacity and transport of pollutants. Furthermore, SOA constitutes up to 30% of simulated organic particulate matter at inland locations, with maximum contributions occurring during afternoon hours. Anthropogenic sources contribute over 90% of simulated SOA at most locations in the basin. Oxidation products of aromatic compounds from anthropogenic sources constitute over 70% of total simulated SOA. Sensitivity runs indicate strong dependence of SOA on VOC emissions and temperature. Overall, model predictions are in qualitative agreement with recent observations in the SoCAB.

Citation: Vutukuru, S., R. J. Griffin, and D. Dabdub (2006), Simulation and analysis of secondary organic aerosol dynamics in the South Coast Air Basin of California, *J. Geophys. Res.*, 111, D10S12, doi:10.1029/2005JD006139.

1. Introduction

[2] Atmospheric particulate matter (PM) is a complex mixture of a large number of inorganic (including water) and organic compounds [Seinfeld and Pandis, 1998]. A significant fraction of organic PM is formed by the physical and chemical transformation of primary gas-phase emissions into secondary organic aerosol (SOA). For example, in the South Coast Air Basin of California (SoCAB) where PM levels are often out of regulatory compliance (California Air Resources Board, http://www.arb.ca.gov/adam/ welcome.html), SOA has been estimated to constitute as much as 80% of total ambient organic PM [Turpin and Huntzicker, 1995]. SOA is formed in the ambient atmosphere through the oxidation of volatile organic compounds (VOCs) and subsequent partitioning of some oxidation products into the aerosol phase. Gas-particle partitioning occurs because of sufficiently low vapor pressure of oxida-

- [3] The contribution of SOA to airborne PM is poorly characterized mainly because of difficulties associated with sampling and chemical analysis of carbonaceous aerosol particles [Turpin et al., 2000]. Further, the dynamics of SOA formation on a regional scale is coupled intricately to spatial and temporal variations of emissions, advective transport by wind, and meteorological conditions. Though simulations of ozone and inorganic aerosols are performed routinely on a regional scale [Seinfeld, 2004], detailed modules that enable SOA simulation on this scale have emerged only recently [Schell et al., 2001; Griffin et al., 2002a, 2002b; Pun et al., 2002; Koo et al., 2003]. In addition to base case studies, such modules also enable the simulation of a variety of scenarios, thereby providing insight into dynamics of SOA formation.
- [4] Studies in the past used models that predict primary organic aerosol (POA) to estimate SOA through the difference between observed and predicted total organic aerosol (OA) concentrations [Harley and Cass, 1994; Strader et al., 1999]. Some regional and global models use adapted SOA yields obtained from chamber experiments to estimate SOA formation [Andersson-Sköld and Simpson, 2001; Chung and Seinfeld, 2002; Tsigaridis and

Copyright 2006 by the American Geophysical Union. 0148-0227/06/2005JD006139\$09.00

D10S12 1 of 13

tion products as compared to that of the parent gas-phase organic species present in anthropogenic and biogenic emissions [*Pankow*, 1994a, 1994b].

¹Department of Mechanical and Aerospace Engineering, University of California, Irvine, California, USA.

²Institute for the Study of Earth, Oceans and Space and Department of Earth Sciences, University of New Hampshire, Durham, New Hampshire, USA

Kanakidou, 2003; Dechapanya et al., 2004; Lack et al., 2004]. The yield, Y, of SOA is defined as

$$Y = \frac{M_o}{\Delta \text{VOC}} \tag{1}$$

where M_o (µg m⁻³) is the mass concentration of SOA produced from the mass concentration of VOC reacted (Δ VOC, µg m⁻³). Assuming that a parent VOC leads to only two overall semivolatile products, *Odum et al.* [1996] developed an empirical framework to fit experimental data from chamber experiments in order to obtain Y as a function of organic aerosol mass concentration. *Sheehan and Bowman* [2001] extended this concept to account for dependence of Y on temperature. This approach allows for modeling SOA formation directly from laboratory data. However, it ignores variability of SOA yield due to changes in oxidant level, and relative humidity (RH).

- [5] SOA modules developed from first principles that explicitly consider gas-phase chemistry of VOCs and thermodynamic properties of partitioning species are more robust and applicable to wide variety of scenarios. Recent advances in this direction include the development of the Caltech Atmospheric Chemistry Mechanism (CACM) [Griffin et al., 2002a] and the Model to Predict the Multiphase Partitioning of Organics (MPMPO) [Pun et al., 2002; Griffin et al., 2003]. The CACM predicts explicitly secondary and tertiary oxidation products of VOCs that potentially form SOA while the MPMPO is the most general thermodynamic module to calculate equilibrium concentrations of organic species across multiple phases.
- [6] This work analyzes in detail the dynamics of SOA formation in the SoCAB by incorporating updated versions of CACM and MPMPO in a three-dimensional air quality model. This is the first modeling study to characterize the formation of SOA in the SoCAB with respect to spatial and temporal variation, oxidation capacity of the atmosphere, chemical composition, nature of origin, and phase distribution of condensible organics between the aerosol and gas phases. Additionally, this paper evaluates the impact of several improvements made to CACM and MPMPO recently by *Griffin et al.* [2005] and presents model sensitivity studies in the context of three-dimensional implementation.
- [7] The host air quality model and the CACM and MPMPO modules are described in section 2. Results of the model are presented in section 3, and sensitivity studies are presented in section 4, followed by the conclusions in section 5.

2. Model Description

2.1. CIT Model

[8] The host CIT air quality model has evolved over the years and used in air quality studies for the SoCAB region in the past [Harley et al., 1993; Harley and Cass, 1994, 1995; Meng et al., 1998; Fraser et al., 2000; Carreras-Sospedra et al., 2005]. The Eulerian CIT model solves governing equations for gas-phase and aerosol-phase species by incorporating detailed mechanisms for advective transport, dry deposition and vertical mixing. Harley et al. [1993] used the CIT model to simulate the 1987 South Coast Air Quality Study (SCAQS) and achieved good

agreement between predicted and observed concentrations for gas-phase species. *Meng et al.* [1998] extended the CIT model to include inorganic aerosol dynamics.

[9] The computational domain consists a grid of 80 horizontal and 30 vertical cells, each 5×5 km in size. The vertical scale of the modeling region extends to 1100 m and is resolved into 5 layers of varying height. Meteorological fields such as temperature, wind, and relative humidity fields are provided as model inputs and usually are developed from observations and diagnostic models. The initial conditions and lateral boundary conditions for model runs are set using field observations. Surface boundary conditions for all species in the model are determined by the net flux between dry deposition and flux due to emissions. A no-flux boundary condition is assumed for the top boundary. The CIT model implements an operator splitting technique [McRae and Seinfeld, 1982] to solve the governing equations numerically by decoupling chemistry, transport, and aerosol dynamics operators. As shown in Figure 1, a schematic of the CIT model, the sequence of operators that are applied on gas-phase and aerosol-phase concentrations are $T_x T_y T_{z,c} T_a T_y T_x$ where T_x , T_y , $T_{z,c}$ and T_a represent the operators of transport in x-direction, transport in y-direction, transport in the z-direction and gas-phase chemistry, and aerosol dynamics respectively. The Ouintic Splines Taylor Series Expansion (QSTSE) algorithm is used to solve the advection equation [Nguyen and Dabdub, 2001]. The condensation/evaporation equation associated with inorganic aerosol dynamics is solved by the Partitioned Flux Integrated Semi-Lagrangian Method (PFISLM) [Nguyen and Dabdub, 2002].

2.2. Production of Secondary Organics From VOCs

[10] The dominant loss process for VOCs in the atmosphere is oxidation, which can result in production of a large number of organic compounds with a variety of functional groups [Atkinson, 1990, 1997; Forstner et al., 1997; Hoffmann et al., 1997; Yu et al., 1999]. A general oxidation reaction of VOCs in the atmosphere can be represented by [Atkinson, 1990, 1997]

$$O_x + VOC \rightarrow \ldots + \alpha_n S_n + \alpha_m S_m + \ldots$$

where O_x is any of the oxidizing radicals (OH, Cl, NO₃) or ozone (O₃), α_n , α_m are stoichiometric factors, and S_n , S_m are products, some of which may be semivolatile or nonvolatile and partition into the aerosol phase. Such products differ widely in their physical and chemical properties as well as their ability to undergo further reactions to produce second and third generation compounds, resulting in an even larger set of compounds [Atkinson, 1990, 1997].

[11] In order to predict SOA concentrations from first principles, one has to consider explicitly all VOCs that undergo oxidation and model comprehensively all chemical pathways that produce SOA precursors. However, the gasphase chemistry of VOCs is complex and not fully understood. Furthermore, the atmospheric oxidation of VOCs produces a large number of organic compounds, and not all of them are known. Notwithstanding the knowledge gaps that exist in terms of reaction rate constants and physical and chemical properties of compounds, such a detailed treatment is computationally infeasible for this type of air

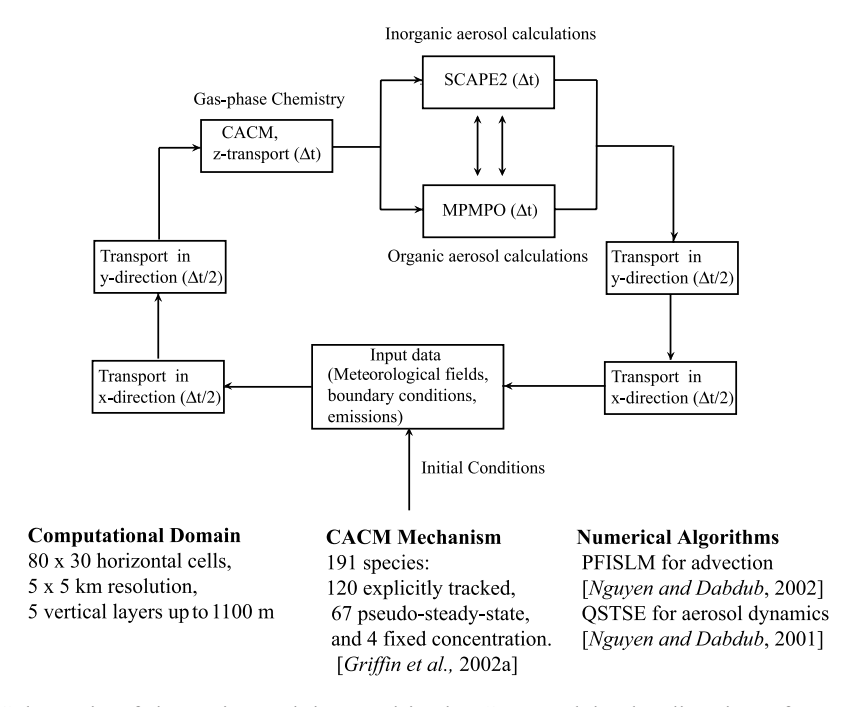


Figure 1. Schematic of the main modules used in the CIT Model. The direction of arrows shows the sequence of operators that are performed on gas and aerosol phase concentrations to solve the governing equations numerically in the CIT model using a symmetrical operator splitting method. Δt is time step for one full iteration.

quality modeling. Consequently, recent approaches to model gas-phase VOC chemistry have lumped similar organic species into groups that are represented by a surrogate compound [Stockwell et al., 1997]. Such lumped mechanisms include the chemistry of surrogate compounds in sufficient detail that the modeling of VOCs gas-phase chemistry is possible.

[12] The CACM chemical mechanism [Griffin et al., 2002a] is used in this study to model the gas-phase chemistry of VOCs. The CACM includes a total of 191 species, of which 120 species are tracked explicitly, 67 are assumed to be pseudo-steady-state species, and 4 have fixed concentrations, as indicated in Figure 1. The concentrations of explicitly tracked species are determined numerically on the basis of kinetics, emissions, and deposition. The inorganic chemistry associated with CACM is based on the Statewide Air Pollution Research Center (SAPRC-99) mechanism of Carter [2000]. In CACM, parent organic compounds are lumped into surrogate groups, each of which is represented by a surrogate compound, as shown in Table 1. The lumping procedure is similar to that of the Regional Atmospheric Chemistry Model (RACM) [Stockwell et al., 1997]. Namely, it is based on functional and structural similarities as well as reactivities. An additional parameter considered in the CACM lumping is the potential of a VOC to form SOA.

[13] Griffin et al. [2005] recently updated CACM to achieve closer agreement between model simulations and experimental results from chamber studies [Odum et al., 1996; Forstner et al., 1997; Hoffmann et al., 1997; Griffin et al., 1999]. The updates to CACM impact the chemistry of aromatic compounds through adjustments to estimated stoichiometric factors and kinetic reaction rate constants.

The updates also achieve a better distinction between high SOA yield (AROH) and low SOA yield (AROL) aromatics [Odum et al., 1997] than the original formulation. Initial evaluation of the updated model shows qualitative agreement between simulated SOA yields of AROL and AROH and data derived from chamber experiments. The updated CACM also includes changes to the chemistry of biogenic compounds to compensate for overprediction of SOA formation and to improve the prediction of the temporal behavior of SOA formation [Hoffmann et al., 1997]. For more details, the reader is referred to Griffin et al. [2005].

2.3. Thermodynamics of SOA Formation

[14] It is hypothesized that the dominant mechanism of gas/particle phase separation of semivolatile organics in the atmosphere is absorption [Pankow, 1994a]. The ambient atmospheric PM acts as an absorbing medium and is a mixture of inorganic (including water) and organic compounds. Despite recent developments [Clegg et al., 2001; Ming and Russell, 2002; Clegg and Seinfeld, 2004], currently no models exist that are capable of determining thermodynamic properties of a general inorganic/organic/ water mixture. Therefore dynamics of the inorganic and organic components of aerosol generally are computed separately. This work incorporates MPMPO to compute the equilibrium concentrations of organic compounds. The dynamics of inorganic aerosol are computed by the module Simulating the Composition of Atmospheric Particles at Equilibrium 2 (SCAPE2) [Kim et al., 1993; Meng et al., 1995, 1998]. The modules are coupled, however, through aerosol properties such as liquid water content (LWC) and pH. POA that is emitted directly into atmosphere also constitutes a significant fraction of ambient PM. For the

Table 1. Parent VOCs Lumped Into Surrogate Groups in the CACM

Surrogate Group		Surrogate Compound
Short-chain alkanes (ALKL) Medium chain alkanes (ALKM) Long-chain alkanes (ALKH)	Alkanes	2-methyl-butane 3,5-dimethyl-heptane <i>n</i> -hexadecane
Short-chain alkenes (OLEL) Long-chain alkenes (OLEH)	Alkenes	1-pentene 4-methyl-1-octene
Low SOA yield aromatics (AROL) High SOA yield aromatics (AROH) Phenolic species (AROO) Aldehydic aromatics (ARAL) Acidic aromatics (ARAC) Polycylic aromatics (PAH) Higher aldehydes (ALD2) Short-chain ketones (KETL) Long-chain ketones (KETH)	Aromatics	1,2,3-trimethyl-benzene 3- n-propyl-toluene 2,6-dimethyl-phenol p-tolualdeyde p-toluic acid 1,2-dimethyl-naphthalene n-pentanal 2-pentanone 2-heptanone
Higher alcohols (ALCH)	Alcohols	2-hexanol
Low SOA yield biogenics (BIOL) High SOA yield biogenics (BIOH)	Biogenics	α-terpineol γ-terpinene

sake of this modeling study, POA is assumed to be chemically inert and remain in the particle phase. However, POA undergoes physical processes such as advective transport, vertical mixing and dry deposition. The integration of MPMPO and SCAPE2 with the CIT model is schematically shown in Figure 1.

[15] Early gas/particle partitioning models for organic species assumed that semivolatile compounds condense to form SOA only if their gas-phase concentrations exceed their saturation vapor pressures [Pandis et al., 1992]. Contrary to this assumption, experimental evidence shows that phase partitioning of semivolatile organic compounds occurs through adsorption on or absorption into a sorbent, even below the saturation pressure [Odum et al., 1996; Saxena and Hildemann, 1996; Liang et al., 1997]. The thermodynamic formalism developed by Pankow [1994a, 1994b] relates the subcooled liquid vapor pressure of semi-volatile organic compounds with gas-phase and particle-phase concentrations and is the basis for the MPMPO module.

[16] The MPMPO assumes a priori that only two aerosol phases exist, one of which is predominantly aqueous and the other of which is predominantly organic. Consequently, the semivolatile organic species distribute themselves among all three phases (gas, organic, and aqueous) to achieve thermodynamic equilibrium. The equilibrium relationship that determines the phase distribution of partitioning compounds between the organic aerosol phase and the gas phase is expressed as [*Pankow*, 1994a, 1994b]

$$K_{om,i} = \frac{A_i}{G_i M_o} \tag{2}$$

where $K_{om,i}$ (m³ µg⁻¹) is the partitioning coefficient for condensing species i and A_i and G_i are its mass

concentrations ($\mu g m^{-3}$) in the organic aerosol phase and the gas phase, respectively. M_o is the total mass concentration ($\mu g m^{-3}$) of an absorbing organic medium. M_o includes POA in addition to semivolatile organics that are already absorbed into the organic aerosol phase. After applying the Ideal Gas Law and Raoult's Law and using molar units for concentration, $K_{om,i}$ can be expressed as

$$K_{om,i} = \frac{RT}{MW_{om}10^6 \gamma_i p_{L,i}^o} \tag{3}$$

where R is the ideal gas constant (8.2 × 10⁻⁵ m³ atm mol⁻¹ K⁻¹, 1 atm = 101.325 KPa), T (K) is absolute temperature, MW_{om} is the average molecular weight of the absorbing phase (g mol⁻¹), $p_{L,i}^O$ (atm) is the pure component vapor pressure of species i, and γ_i is the activity coefficient of species i in the organic phase. The factor 10^6 converts g to μg .

[17] The gas/particle phase equilibrium for species in an aqueous aerosol phase is governed by

$$AQ_i = \frac{G_i(LWC)HL_i}{\gamma_{aq,i}} \tag{4}$$

where AQ_i is the aqueous aerosol-phase concentration of species i (µg m⁻³), HL_i is its Henry's Law coefficient ((µg µg⁻¹ H₂O)/(µg m⁻³ air)), LWC is the aerosol liquid water content (µg H₂O m⁻³ air), and $\gamma_{aq,i}$ is the activity coefficient of species i in the aqueous aerosol phase, normalized by that at infinite dilution. The UNIFAC model [Fredenslund et al., 1977] is used to estimate activity coefficients. The equilibrium concentrations of partitioning species that dissociate in the aqueous phase are also governed by an additional set of equations describing equilibrium dissociation.

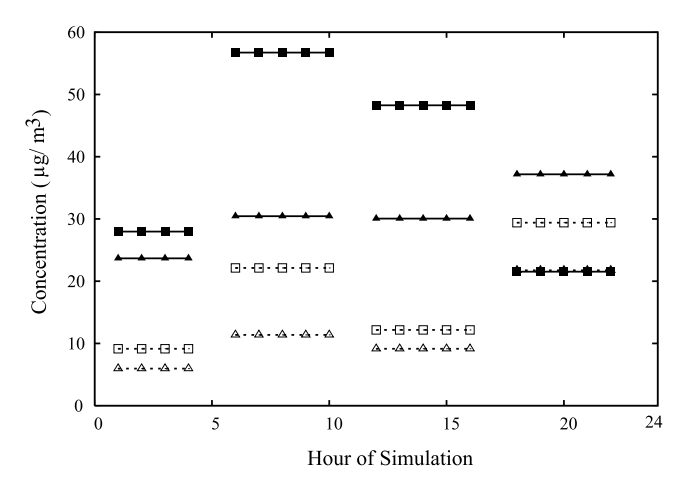


Figure 2. Comparison of observed (solid symbols) and predicted (open symbols) organic aerosol concentrations for central Los Angeles (squares) and Claremont (triangles). Open triangles and solid squares overlap toward the end of the simulation.

[18] An iterative solution to equations (2) through (4) achieves simultaneous equilibrium concentrations of partitioning species among the organic aerosol phase, the aqueous aerosol phase, and the gas phase. The solution is also constrained by the total mass of semivolatile species predicted by CACM and dissociation in the aqueous phase. There are over 60 species that are identified as semivolatile and thus capable of partitioning into the aerosol phase. However, computational demands and lack of thermodynamic data require a simplified treatment.

[19] The semivolatile gas-phase SOA precursors are lumped into 10 surrogate groups on the basis of the nature of the origin of their parent compound (anthropogenic or biogenic), structure, volatility, and dissociative capability. The thermodynamic behavior of each surrogate group is characterized by properties of a representative compound. The original version of MPMPO classified surrogate species on the basis of their affinity toward water [*Pun et al.*, 2002]. Consequently, groups that are classified as hydrophilic are forced to partition only into an aqueous phase, and groups that are classified as hydrophobic are partitioned only into an organic phase. This model artifact rendered the original formulation partly insensitive toward influence of relative humidity on gas/particle partitioning [*Saxena et al.*, 1995; *Xiong et al.*, 1998].

[20] However, the updated version of MPMPO is incorporated into CIT model for this study. The main feature of the updated model is that all species are simultaneously partitioned into both aqueous and organic phases [Griffin et al., 2003]. This improvement enables a more realistic treatment of gas/particle partitioning. Other updates to the original formulation of MPMPO include a new group to accommodate biogenic ring-retaining compounds, a reclassification of certain compounds, and adjustments to the vapor pressures of SOA surrogates. The adjustments are based on averaging the vapor pressures derived from the two-product fit for individual aromatics or individual monoterpenes in chamber experiments [Odum et al., 1996; Hoffmann et al., 1997; Griffin et al., 1999]. The details of vapor pressure correction, adjustments to thermodynamic

properties, and species reclassification are discussed by *Griffin et al.* [2005].

3. Model Results

3.1. September 1993 Episode

[21] This study uses a 2-day episode that occurred on 8–9 September 1993 to analyze the dynamics of SOA formation in the SoCAB. The input data required are developed from a specialized monitoring campaign conducted from 28 August to 13 September in the SoCAB during the summer of 1993 [Fraser et al., 1996, 1999, 2000].

[22] Emission inventories (both gas and particle phase) are obtained from the South Coast Air Quality Management District (SCAQMD). The POA species present in emission inventories are further classified into eight surrogate groups by MPMPO: *n*-alkanes, PAH, diacids, aliphatic acids, substituted PAH, resolved polycyclic species, substituted monoaromatics, and unresolved organic matter. Each of the surrogate groups are represented by a surrogate compound for the purposes of calculating thermodynamic properties [*Griffin et al.*, 2002b].

[23] Figure 2 compares total organic aerosol predicted by the model against the observed data for two locations in the SoCAB, Claremont and central Los Angeles. A factor of 1.4 [Gray et al., 1984] is used to convert observed OC concentrations presented by Fraser et al. [1996] into organic aerosol (OA) mass to account for the noncarbon mass. The factor of 1.4 is probably more accurate for central Los Angeles because of significant POA contribution. This factor could be higher for Claremont (a downwind site), most likely during afternoon hours, because of high contributions from secondary organics. However, the factor 1.4 is used to remain consistent throughout the model time and space domain and to remain consistent with the source of observations data. Therefore uncertainty in the conversion factor might result in higher than assumed OA concentration at Claremont. The model underpredicts organic aerosol at both locations in comparison with observations. The underpredictions are largely attributed to significant uncertainties that are associated with POA and VOC emission inventories as well as gaps in our understanding of SOA formation processes.

[24] The underpredictions from the model are more pronounced for central Los Angeles as compared to Claremont. Most of the organic aerosol at central Los Angeles is primary in nature owing to large direct emissions. Therefore one possible explanation for underprediction is inaccuracies in the POA emissions inventory. Further, higher POA may lead to higher condensation of SOA as semivolatile organics are absorbed into the available organic medium. Consequently, underprediction of POA may reduce SOA formation, leading to overall underprediction of organic aerosol. Figure 2 also indicates organic aerosol is overpredicted toward the end of the day for central Los Angeles. This may be caused by an under estimate of nighttime vertical turbulent mixing in the model. This anomaly could also be due to a temporal shift in the POA emissions inventory.

[25] Uncertainties in VOC emissions also contribute to underpredictions of organic aerosol, especially at downwind sites, because of secondary contributions. Since SOA formation depends strongly on spatial and temporal evolution

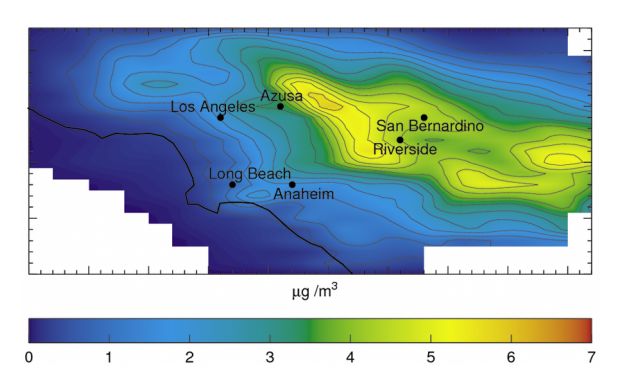


Figure 3. Simulated 24-hour-average SOA concentration levels in the SoCAB for 9 September 1993. The distance between tick marks is 5 km in both horizontal and vertical directions.

of VOC emissions, the accuracy in emissions resolution also plays a role. For example, any missing high yield VOCs at downwind locations during afternoon hours reduce SOA formation. Therefore underprediction at Claremont site, to some extent, may be attributed to any missing sources in the VOC emissions inventory.

[26] Some mechanistic explanations are also possible for underprediction of SOA and hence total organics. For example, aerosol-phase chemistry that potentially increases SOA formation is not accounted for in the current models [Jang et al., 2002; Kalberer et al., 2004]. Compounds that are not considered by CACM, such as sesquiterpenes, contribute significantly to SOA.

3.2. SOA Dynamics in Southern California

[27] In the SoCAB, urban areas around Los Angeles, Long Beach, and Anaheim are significant sources of NO_x, VOCs, and POA. These areas are closer to the coast and encompass high industrial activity and heavily transited freeways. Wind typically blows from west to east, transporting the pollutants to inland areas. Figure 3 shows the predicted 24-houraverage SOA concentration in the SoCAB for 9 September 1993, the second day of simulation. Inland/downwind areas are predicted to experience higher levels of SOA than coastal/upwind areas. The predicted 24-hour-average SOA concentrations at Azusa, Riverside, and San Bernardino (downwind sites) are 3.32, 4.19 and 4.51 μ g m⁻³, respectively. However, the corresponding values at central Los Angeles, Long Beach, and Anaheim (upwind sites) are 1.98, 0.88 and $1.70 \mu g m^{-3}$, respectively. Relatively high SOA concentrations at inland sites are attributed to advective transport of POA, VOCs, oxidation products of VOCs, and SOA itself from coastal sites.

[28] These model results are in qualitative agreement with measurement studies that analyzed PM composition in the SoCAB using the ratio of organic carbon (OC) to elemental carbon (EC) [Kim et al., 2002; Na et al., 2004; Sardar et al., 2005]. The ratio of OC to EC is often used to quantify relative contribution from primary and secondary sources to organic PM [Turpin and Huntzicker, 1991, 1995; Cabada et al., 2004; Millet et al., 2005]. EC results from combustion processes and acts as a tracer of primary emissions. OC to EC ratio values between 2 and 5 are generally representative of OA that is mostly primary in nature [Strader et al., 1999].

Higher OC to EC ratios than those assumed for primary emissions is attributed to the formation of SOA.

[29] Sardar et al. [2005] observed that inland sites with in the SoCAB presented a higher OC to EC ratio in PM_{2.5} than did coastal sites. From data collected over several months, the average OC to EC ratios at Riverside and Claremont (inland sites) are 7.49 and 10.6, respectively. The corresponding ratios for Downey and USC (downtown Los Angeles) are 3.63 and 5.07, respectively. Higher measured OC to EC ratios correlate with higher levels of predicted SOA at downwind sites, as shown in Figure 3.

[30] Further, the OC mass concentration at Claremont (an inland site) in the ultrafine mode is higher in summer months than it is in winter months [Sardar et al., 2005]. Advective transport of pollutants from coastal to inland areas is more pronounced in summer because of increased wind speeds [Kim et al., 2002]. Therefore SOA formation in downwind sites in summer months is attributed to advective transport. Kim et al. [2002] observed similar seasonal variation and concluded that a substantial fraction of ultrafine particles is formed from secondary processes in summer months at Riverside.

3.2.1. Diurnal Variation

[31] The predicted diurnal variation of SOA for the second day of simulation is shown for six locations in Figure 4. Urban locations show significant diurnal variation with peaks in SOA concentration occurring during morning hours. The peak concentration at central Los Angeles is 6.64 μg m⁻³ and occurs around 1100 hours while the 24-hour-average is 1.98 μg m⁻³. VOC and POA emissions that are highest in morning hours because of automobile traffic lead to the peak late morning SOA concentrations. Predicted peak SOA concentrations at Anaheim and Long Beach are 5.05 and 2.15 μg m⁻³, respectively, and occur at 1000 hours. Peak concentrations at coastal locations are significantly higher than 24-hour-average concentrations. SOA levels decrease later in the day because of the decrease in transport and in oxidation capacity with photochemical activity.

[32] Predicted peak concentrations for inland sites are similar to those at coastal locations. However, in contrast to coastal areas, inland sites such as Riverside, San Bernardino, and Azusa are predicted to experience higher sustained SOA concentrations. The peak concentration at San Bernardino is $6.56~\mu g~m^{-3}$ and occurs around 1100 hours while the 24-hour-average is $4.51~\mu g~m^{-3}$. Local emissions may lead to peak SOA levels during morning hours. High SOA concentrations during early morning hours at some inland locations, such as at Riverside as shown in Figure 4, is due to certain meteorological conditions such as low mixing height and low temperature. The peak concentration at Riverside is $5.35~\mu g~m^{-3}$ and occurs at 600 hours. Azusa experiences peak SOA concentration of $5.55~\mu g~m^{-3}$ at 1000 hours.

3.2.2. Contribution of SOA to Simulated Total Organic PM

[33] Similar trends to those shown in Figure 4 are observed when considering the simulated contribution of SOA to the total organic component of ambient PM. Predicted SOA constitutes a higher percentage of total predicted organics at inland locations compared to coastal locations. The peak percentage contribution of SOA to total organics in the aerosol phase is 30% at Azusa, while it is 19% at central Los Angeles, as shown in Figure 5. POA

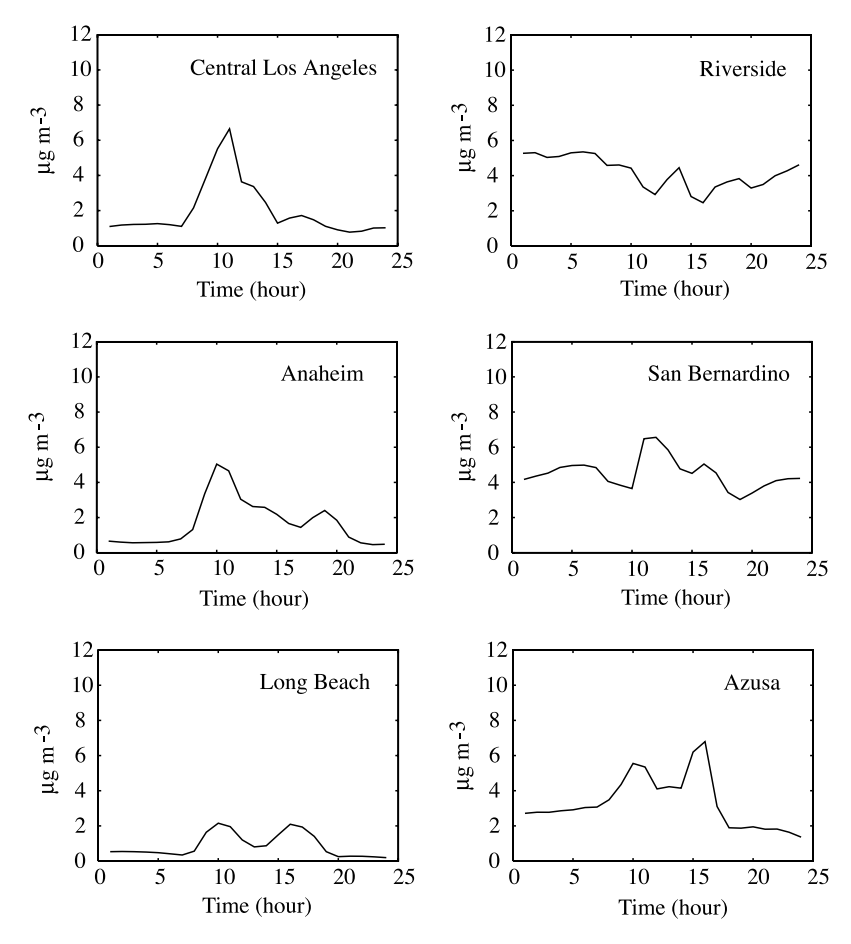


Figure 4. Simulated diurnal variation of SOA concentration levels at six locations in the SoCAB for 9 September 1993. Central Los Angeles, Long Beach, and Anaheim are major VOC emission sites located upwind with peaks in SOA concentrations in morning hours. Azusa, Riverside, and San Bernardino are downwind locations with higher sustained SOA concentrations.

deposits faster than VOCs. Therefore less POA is transported downwind relative to VOCs that may act as SOA precursors. Therefore urban locations are predicted to contain organic PM composed mostly of POA while downwind locations have more significant contributions from secondary organics. This is observed despite similar peak SOA concentrations at both coastal and inland locations.

- [34] The peaks in organic PM occur during morning hours are due to elevated POA emissions. However, at all locations, SOA constitutes a high percentage of organic PM during afternoon hours because of peak photochemical activity. The peak contribution of SOA to organic PM occurs at 1500 hours for Azusa and at 1300 hours for central Los Angeles as shown in Figure 5.
- [35] Sardar et al. [2005] observed that coastal sites present a stronger correlation between OC and EC for PM_{2.5} than do downwind sites. The stronger correlation between OC and EC for coastal sites indicates the high proportion of PM from POA sources. Kim et al. [2002] also concluded that primary emissions contribute significantly to ultrafine PM at Downey (coastal site).

3.2.3. Production and Partitioning of Condensible Organics

[36] The total amount of condensible organic gases (COGs) formed from the oxidation of VOCs is a measure

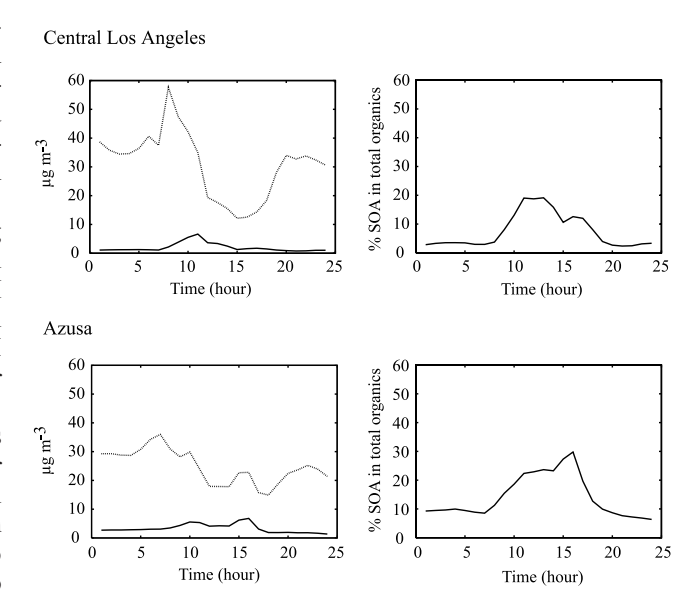


Figure 5. (left) Simulated diurnal variation of organic aerosol (dotted line) and SOA (solid line) for 9 September 1993 in central Los Angeles and Azusa. (right) Percentage contribution of SOA to total organic PM for the same locations.

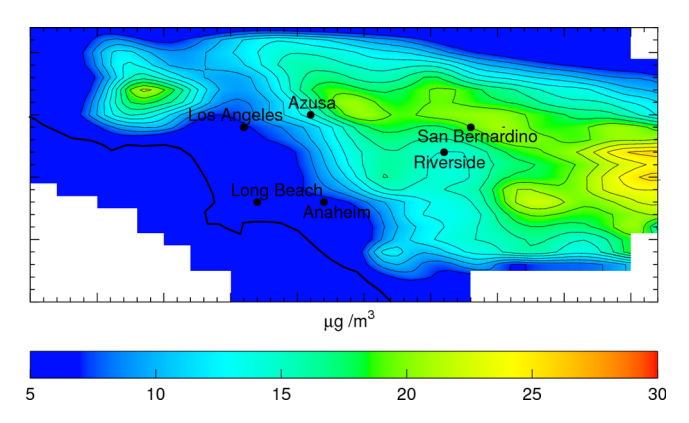


Figure 6. Simulated 24-hour-average concentration levels of COGs for 9 September 1993 in the SoCAB. The distance between tick marks is 5 km in both horizontal and vertical directions.

of SOA-forming potential at a particular location. The total concentration of COGs is defined as the sum concentrations of semivolatile organic compounds existing in both the particle and gas phases. For this study COG concentrations are based on the 10 surrogates used in MPMPO. Figure 6 shows predicted 24-hour-average concentration of COGs on the second day of simulation. The concentration of COGs is higher in inland locations compared to coastal locations because of both local production and transport. The predicted 24-hour-average COG concentrations at central Los Angeles, Long Beach, and Anaheim are 6.79, 3.81, and 5.83 $\mu g \ m^{-3}$, respectively. However, the corresponding values at Azusa, Riverside, and San Bernardino are 13.7, 15.1, and 19.5 $\mu g \ m^{-3}$, respectively. This corresponds to high 24-houraverage SOA for inland sites as shown in Figure 3.

[37] The COG concentration (and thus SOA) strongly depends on the oxidative capacity of the atmosphere, which is primarily determined by O₃. O₃ directly oxidizes alkenes and influences oxidation of other VOCs through formation of OH and NO₃. The measurements from the Pittsburgh Air Quality Study show a strong correlation between the ozone mixing ratio and SOA concentration (based on the OC/EC ratio technique) [Cabada et al., 2004]. Figure 7 shows predicted diurnal variation of O₃, COGs, SOA, and percentage of COGs partitioning into the aerosol phase for central Los Angeles and Azusa. The peak O₃ mixing ratio at Azusa is 250 ppb, and the corresponding value at central Los Angeles is 130 ppb. Mixing ratios of O₃ are considerably higher at Azusa than those predicted at central Los Angeles, and thus the oxidative capacity is as well. Consequently, COGs and SOA are present in higher concentrations at Azusa compared to central Los Angeles. Therefore it is likely that SOA levels at downwind locations are higher than those at coastal locations because of transport of VOCs, POA, and SOA from upwind areas and because of the relatively high oxidative capacity of downwind areas.

3.3. Chemical Composition and Origin of SOA

[38] A species-resolved SOA model has the capability to predict the chemical composition of SOA and characterize it according to the urban/regional emissions profile. Therefore speciation of SOA enables the design of general effective control strategies by identifying classes of VOCs that

contribute most to ambient SOA levels. At this level of detail, however, source specific emissions controls cannot be addressed.

[39] In the SoCAB, anthropogenic emissions rates are much larger than those for biogenic compounds, and this is reflected in the composition profile of SOA. The SOA from oxidation products of anthropogenic VOCs constitute over 90% of the predicted mass for most locations in the basin. Anthropogenic SOA constitutes high percentages in coastal areas of the basin such as Los Angeles (97%) and Anaheim (97%). This fraction decreases slightly for inland locations such as Riverside (94%) and San Bernardino (97%). Biogenic SOA may increase for inland areas because of increased emissions of monoterpenes downwind, as show in the emission maps described by *Carreras-Sospedra et al.* [2005].

[40] As mentioned previously MPMPO lumps SOAforming species into 10 surrogate groups. Table 2 presents general characteristics of compounds lumped into these groups along with their origin (anthropogenic or biogenic) and percentage contribution to 24-hour-average SOA composition. Oxidation products of aromatic compounds form a major component of SOA in the SoCAB due to their high carbon number and the presence of acidic functional groups. Dissociative aromatic fragments constitute 75% of SOA at central Los Angeles, 78% at Claremont, and 68% at Riverside. This results from gas-phase aromatic compounds, main constituents of motor vehicle emissions, being present in high mixing ratios in the SoCAB. Other species that constitute at least 1% on average of SOA in at least one of the locations shown include low-carbon-number compounds, dissociative and nondissociative fragments of biogenics, low volatility ring-retaining aromatics, and longchain alkane oxidation products.

3.4. Comparison With Previous Version of the Model

[41] A comparative study of SOA models by *Pun et al.* [2003] showed that the original formulations of CACM and MPMPO predict relatively high mass concentrations of COGs and SOA. This observation was attributed to the explicit tracking of second and third generation oxidation products in CACM mechanism. However, as discussed in previous sections, *Griffin et al.* [2005] recently made several improvements to original versions of CACM and MPMPO that are expected to impact predicted SOA concentrations. In this section, the original formulation and updated versions are compared using identical set of model inputs. The updated models predict decreases in SOA concentrations, on average by a factor of 3, compared to the first generation modules.

[42] Figure 8 compares predicted concentrations of COGs and SOA for the original and current models at Claremont. The concentration of COGs for the current models ranged from $12-27~\mu g~m^{-3}$ while the same for the original models is $13-45~\mu g~m^{-3}$. The decrease in production of COGs is due to removal of certain highly reactive species from consideration of gas/particle partitioning and to adjustments of stoichiometric factors, mostly to the aromatic chemistry.

[43] The fraction of COGs that exists in the aerosol phase decreased significantly for the current models, as shown in Figure 8, leading to the overall decrease in predicted SOA concentrations. The original models predict the fraction of COGs in the aerosol phase to be as high as 93%. However,

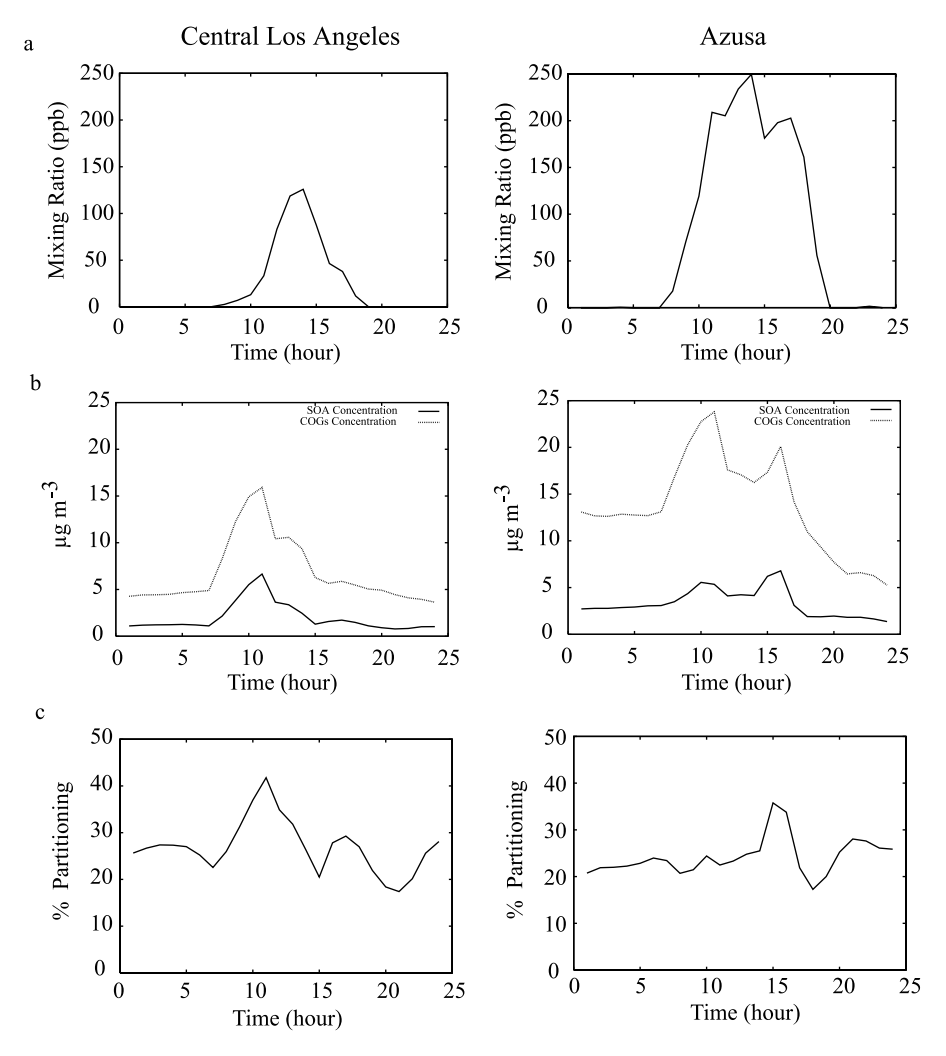


Figure 7. Influence of oxidation capacity on SOA formation. (a) Diurnal variation of simulated ozone in central Los Angeles and Azusa for 9 September 1993. (b) Corresponding values for COGs (dotted line) and SOA (solid line). (c) Percentage of total COGs partitioned into the aerosol phase.

adjustments to vapor pressures and reclassification of species into surrogate groups lead to a decrease in the fraction of COGs that exist in particles. It is suspected that the reclassification of species has a larger effect [Griffin et al., 2005]. The updated model increases the underprediction of total organic aerosol in comparison with the observations in Figure 2. However, the improved model eliminates any compensatory errors present in the original formulation. For

instance, any missing sources of VOCs or POA may been compensated for by the high yield of some VOCs calculated by the previous model.

4. Model Sensitivity

[44] The formation of SOA occurs through a complex series of chemical and physical transformations and strongly

Table 2. Twenty-Four-Hour-Average SOA Composition for 10 Surrogate Groups Lumped on the Basis of Nature of Origin and Functional/Structural Characteristics at Central Los Angeles, Claremont, and Riverside for 9 September 1993

	Origin		Percentage Contribution of Surrogate to SOA		
Surrogate		Characteristics	Central Los Angeles	Claremont	Riverside
S1	anthropogenic	low carbon number	13	3.1	6.4
S2	anthropogenic	aromatic fragments, dissociative	75	78	68
S3	anthropogenic	aromatic fragments, nondissociative	0.18	0.02	0.01
S4	biogenic	dissociative	1.9	0.49	1.1
S5	biogenic	nondissociative	0.68	1.6	5.4
S6	anthropogenic	aromatic, benzene-based, low volatility	3.8	13	15
S7	anthropogenic	aromatic, benzene-based, high volatility	0.46	0.49	0.98
S8	anthropogenic	polyaromatic, naphthalene-based	0.98	0.42	0.28
S9	anthropogenic	alkane-derived	4.3	3.7	2.4
S10	biogenic	ring-retaining	0.04	0.01	0.03

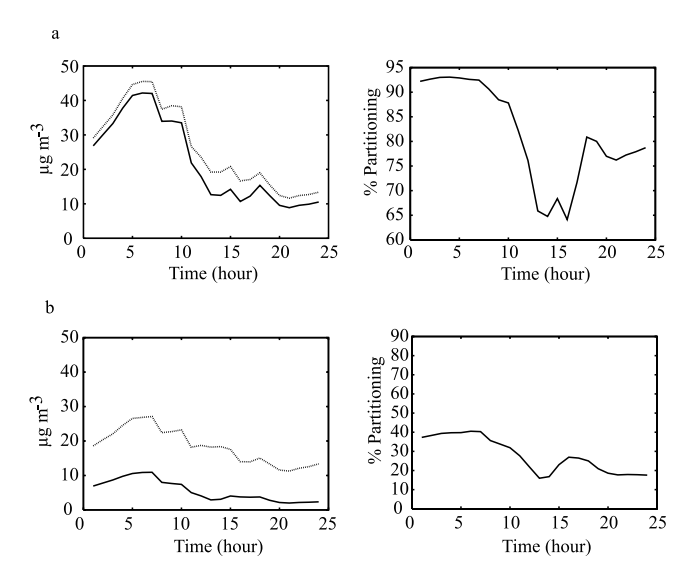


Figure 8. Comparison of (a) original and (b) updated versions of the CACM and the MPMPO modules for predicted COGs (dotted line) and SOA (solid line) for 9 September 1993 at Claremont (left plots). Also shown is corresponding percentage partitioning of COGs into aerosol phase (right plots).

depends on several parameters. This section presents sensitivity of the CACM and MPMPO modules to emissions and meteorological input parameters in the context of three-dimensional implementation using the CIT model.

4.1. Emissions

[45] The emissions of VOCs and NO_x are increased or decreased by a constant factor throughout the basin with respect to base case emissions of the 8–9 September 1993 episode to quantify the dependence of SOA formation on these parameters. As stated previously, VOC emissions lead to the formation of SOA via their atmospheric oxidation. The oxidative capacity of the atmosphere indirectly depends on both VOC and NO_x emissions through the O_3 cycle. Therefore emissions of both VOCs and NO_x are expected to impact SOA formation.

4.1.1. VOCs

[46] A detailed study by Carreras-Sospedra et al. [2005] used the original formulations of CACM and MPMPO to quantify the SOA forming potential of groups of parent VOCs in terms of incremental reactivities. In the current work, a few scenarios are simulated to study the sensitivity of the updated versions of the models by considering both COGs and SOA. The 24-hour-average simulated COG and SOA concentrations as a function of percentage of base case VOC emissions are shown in Figure 9 for central Los Angeles and Azusa. For example, a 20% increase in VOC emissions over the base case leads to increase in COGs by $0.89 \mu g m^{-3}$ and in SOA by $0.32 \mu g m^{-3}$ at central Los Angeles. The production of condensible organics increases with VOCs, as expected. SOA concentrations also increase with VOCs indicating the semivolatile nature of the COGs. The increase in secondary organics with respect to the increase in VOC emissions is greater for Azusa because of both higher oxidation capacity at and transport to this location.

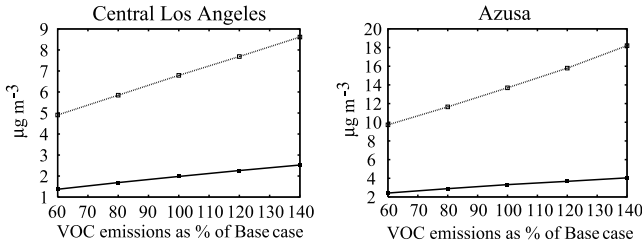
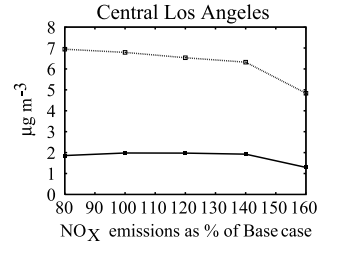


Figure 9. Predicted 24-hour-average concentrations of COG (dotted line) and SOA (solid line) as a function of percentage of base case VOC emissions for 9 September 1993 for central Los Angeles and Azusa.

4.1.2. Nitrogen Oxide Emissions

[47] The formation of SOA depends on NO_x through the gas-phase chemistry of VOCs and O_3 . NO_x emissions are primarily responsible for the production of O_3 , which strongly determines the extent of oxidation of parent VOCs, and thus the production of COGs. The CACM explicitly incorporates oxidation reactions of parent VOCs through the chemistry of surrogate compounds. Hence the influence of NOx on SOA formation is sensitive to changes in oxidant levels and changes in chemical reactions that occur. The SoCAB is a NO_x -rich region, and an increase in NO_x results in a decrease of O_3 because HO_x - NO_x reactions dominate over HO_x - HO_x reactions [*Griffin et al.*, 2004].

[48] Figure 10 shows simulated concentrations of COG and SOA as a function of percentage of base case NO_x emissions for central Los Angeles and Azusa. As expected, increases in NO_x emissions lead to decreases in the production of COGs because of the concurrent decrease in O₃. An increase in NOx emissions by 20% results in a decrease of 24-hour-average COG concentration at central Los Angeles from 6.79 to 6.53 μg m⁻³ and at Azusa from 13.7 to 13.1 μ g m⁻³. NO_x also influences gas/particle partitioning to the aqueous phase through concentrations of inorganic compounds such as aerosol nitrate. This effect potentially results in increases in SOA concentration with the increases in NO_x emissions. [Pun et al., 2002]. However, only a limited impact of NO_x is observed on predicted SOA concentrations in the current models. It may also be possible that the more volatile constituents of COGs (those that are less likely to form SOA) are affected by NOx level to a greater degree than those constituents of COGs that are less volatile.



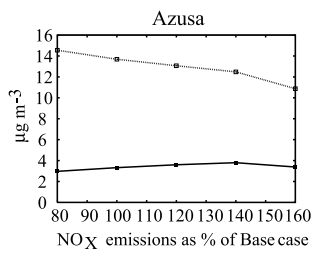


Figure 10. Predicted 24-hour-average concentrations of COG (dotted line) and SOA (solid line) as a function of percentage of base case NO_x emissions for 9 September 1993 at central Los Angeles and Azusa.

10

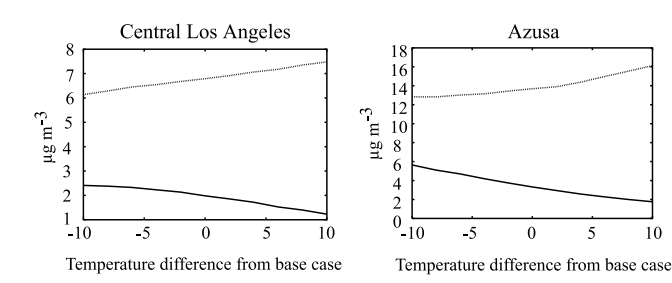


Figure 11. Predicted 24-hour-average concentrations of COG (dotted line) and SOA (solid line) as a function of temperature for 9 September 1993 at central Los Angeles and Azusa. Temperature is shown as difference from the base case.

4.2. Meteorological Parameters

[49] Meteorological conditions play a key role in the formation of SOA, as is evident from the seasonal and diurnal variations of SOA [Millet et al., 2005; Lack et al., 2004]. For example, temperature directly influences SOA formation. Mixing height has an indirect effect on SOA through mixing volume of precursors and oxidants. Relative humidity (RH) affects the LWC of the aqueous aerosol into which SOA species may partition.

4.2.1. Temperature

[50] The rates of gas-phase chemical reactions are strongly dependent on temperature. Further, for condensible organics, vapor pressures also depend on temperature. Therefore SOA is expected to be a strong function of temperature, as has been shown in box modeling studies and chamber studies [Griffin et al., 2005; Takekawa et al., 2003; Sheehan and Bowman, 2001]. However, less work has been performed on temperature effects using a three-dimensional modeling framework [Strader et al., 1999; Aw and *Kleeman*, 2003].

[51] Figure 11 shows the concentrations of COGs and SOA versus temperature for central Los Angeles and Azusa. Other parameters such as emissions, RH, and mixing heights are those from the base case. The concentration of COGs increases with temperature, as oxidation rates of VOCs increase with temperature, leading to the increased production of secondary organics. However, the increase in temperature has an opposite effect on the formation of SOA. Concentrations of SOA decrease with increases in temperature because the vapor pressure of condensible organics increase with temperature. Therefore less mass partitions into the aerosol phase. The dependence of SOA on temperature concentration is consistent with other studies [Aw and Kleeman, 2003], but no optimum temperature for SOA formation is observed in the range of the base case temperatures ±10°C for the September 1993 episode. Such an optimal temperature was observed by Strader et al. [1999] for the San Joaquin Valley.

4.2.2. Mixing Height

[52] Mixing height influences the formation of SOA via vertical mixing of precursors and oxidants. Decreasing the mixing height by 20% throughout the basin leads to an increase in 24-hour-average concentration of SOA at central Los Angeles by 11.5%, from 1.98 to 2.21 μ g m⁻³, and at Azusa by 20.2%, from 3.32 to 4.00 μ g m⁻³. Lower mixing

heights lead to the accumulation of both precursors and SOA. The opposite trend is observed for an increase in mixing height. The 24-hour-average concentration of SOA decreases at central Los Angeles by 10.4%, from 1.98 to 1.88 $\mu g \text{ m}^{-3}$, and at Azusa by 24.6%, from 3.32 to $2.86 \ \mu g \ m^{-3}$.

4.2.3. Relative Humidity

[53] Two scenarios that increase RH by a factor of 1.4 or decrease RH by a factor of 0.6 with respect to base case values do not show any significant difference in total SOA formation. However, it is likely that RH affects the phase distribution of SOA between aqueous and organic phases without a significant impact on total SOA formation, as has been observed in some box modeling studies [Griffin et al., 2003]. Further, data from the Pittsburgh supersite show no correlation between SOA formation (based on the OC/EC ratio technique) and RH [Cabada et al., 2004].

5. Conclusions

[54] In this study, the CACM mechanism is coupled with the MPMPO module in a three-dimensional air quality model to characterize SOA formation in the SoCAB region. CACM and MPMPO represent the current state-of-science in predictive SOA modeling. A 2-day episode that occurred on 8-9 September 1993 is used for this purpose. Model results support the following conclusions.

[55] Inland locations in the SoCAB experience higher levels of SOA compared to coastal locations because of advective transport of pollutants from upwind areas. In addition to transport, the oxidative capacity of the atmosphere also determines the spatial distribution of SOA in this region. Relatively high oxidative capacity leads to a greater production of COGs at inland sites than at coastal sites. Overall, this results in SOA contributing up to 35% of simulated organic PM at inland sites. Organic PM at coastal sites is mostly primary in nature.

[56] Coastal locations show a strong diurnal variation in SOA concentrations. Peak concentrations at coastal locations are significantly higher than 24-hour-average concentrations and occur during late morning hours. In comparison with coastal sites, inland sites present a higher base line for SOA concentrations, although peak concentrations are similar to those at coastal locations. Some inland sites show peaks of SOA during morning hours due to local emissions.

[57] Anthropogenic sources contribute over 90% of SOA at most locations in the SoCAB. Further speciation using 10 surrogate groups from MPMPO shows that aromatic fragments dominate simulated SOA composition in this region because of their high carbon number, low vapor pressure (associated with acidic functional groups), and high emission rates for precursor compounds.

[58] Model sensitivity studies show a strong dependence of SOA formation on emission and meteorological parameters. Temperature plays a key role in the SOA formation process. Overall, SOA decreases with increases in temperature, although production of semivolatile organic compounds increases with temperature. VOC and NO_x emissions influence SOA concentrations through gas-phase chemistry. While VOC emissions impact available precursor compounds that oxidize and form SOA, both VOC and NO_x determine oxidation capacity of the atmosphere through O_3 mixing ratio.

[59] Model results are in qualitative agreement with measurement studies for the SoCAB region, although SOA modules used in this study are limited by current understanding of SOA formation processes. Given the complex nature of the formation mechanisms involved, SOA simulation is a challenging aspect of atmospheric aerosol modeling. The findings from this study and similar analyses for other regions will be of importance toward developing strategies to reduce particulate pollution. Furthermore, results presented here provide guidance for the design of future field studies.

[60] Acknowledgments. This study has been supported by the CAREER Award Grant ATM-9985025 from the National Science Foundation to D.D. Any opinions, findings, and conclusions or recommendations expressed in this publication are those of the authors and do not necessarily reflect the views of the National Science Foundation. This work was also performed, in part (RJG), under STAR Research Assistance Agreement R831083 awarded by the U.S. Environmental Protection Agency (EPA) through a subcontract from the University of California at Davis. It has not been formally reviewed by EPA. The views expressed in this document are solely those of the authors, and EPA does not endorse any products or commercial services mentioned in this publication.

References

- Andersson-Sköld, Y., and D. Simpson (2001), Secondary organic aerosol formation in northern Europe: A model study, J. Geophys. Res., 106, 7357-7374.
- Atkinson, R. (1990), Gas-phase tropospheric chemistry of organic compounds: A review, Atmos. Environ., Part A, 24, 1-41.
- Atkinson, R. (1997), Gas-phase tropospheric chemistry of volatile organic compounds. 1. Alkanes and alkenes, *J. Phys. Chem. Ref. Data*, 26, 215–290.
- Aw, J., and M. J. Kleeman (2003), Evaluating the first-order effect of intraannual temperature variability on urban air pollution, *J. Geophys. Res.*, 108(D12), 4365, doi:10.1029/2002JD002688.
- Cabada, J. C., S. N. Pandis, R. Subramanian, A. L. Robinson, A. Polidori, and B. Turpin (2004), Estimating the secondary organic aerosol contribution to PM_{2.5} using the EC tracer method, *Aerosol Sci. Technol.*, 38, 140–155, doi:10.1080/02786820390229084.
- Carreras-Sospedra, M., R. J. Griffin, and D. Dabdub (2005), Calculations of incremental secondary organic aerosol reactivity, *Environ. Sci. Technol.*, 39, 1724–1730.
- Carter, W. P. L. (2000), Documentation of the SAPRC-99 chemical mechanism for VOC reactivity assessment, final report, Calif. Air Resour. Board, Sacramento.
- Chung, S., and J. H. Seinfeld (2002), Global distribution and climate forcing of carbonaceous aerosols, *J. Geophys. Res.*, 107(D19), 4407, doi:10.1029/2001JD001397.
- Clegg, S. L., and J. H. Seinfeld (2004), Improvement of Zdanovskii-Robinson-Stokes model for mixtures containing solutes of different charge types, *J. Phys. Chem.*, 108, 1008–1017.
- Clegg, S. L., J. H. Seinfeld, and P. Brimblecombe (2001), Thermodynamic modeling of aqueous aerosols containing electrolytes and dissolved organic compounds, J. Aerosol. Sci., 32, 713–738.
- Dechapanya, W., M. Russell, and D. T. Allen (2004), Estimates of anthropogenic secondary organic aerosol formation in Houston, Texas, *Aerosol Sci. Technol.*, 38, 156–166.
- Forstner, H. J. L., R. C. Flagan, and J. H. Seinfeld (1997), Secondary organic aerosol from photooxidation of aromatic hydrocarbons: Molecular composition, *Environ. Sci. Technol.*, *31*, 1345–1358.
- Fraser, M. P., D. Grosjean, E. Grosjean, E. Rasumussen, and R. A. Cass (1996), Air quality model evaluation data for organics. 1. Bulk chemical composition and gas/particle distribution factors, *Environ. Sci. Technol.*, 30, 1731–1743.
- Fraser, M. P., G. R. Cass, and B. R. T. Simoneit (1999), Particulate organic compounds emitted from motor vehicle exhaust and in the urban atmosphere, *Atmos. Environ.*, 33, 2715–2724.
- Fraser, M. P., M. J. Kleeman, J. J. Schauer, and G. R. Cass (2000), Modeling the atmospheric concentrations of individual gas-phase and particle-phase organic compounds, *Environ. Sci. Technol.*, 34, 1302–1312.
- Fredenslund, A., J. Gmehling, and P. Rasmussen (1977), Vapor-Liquid Equilibrium Using UNIFAC, Elsevier, New York.

- Gray, H. A., G. R. Cass, J. J. Huntzicker, E. Heyerdahl, and J. A. Rau (1984), Characterization of atmospheric organic and elemental carbon particle concentrations in Los Angeles, *Sci. Total Environ.*, *36*, 17–25.
- Griffin, R. J., D. R. Cocker III, R. C. Flagan, and J. H. Seinfeld (1999), Organic aerosol formation from the oxidation of biogenic hydrocarbons, *J. Geophys. Res.*, 104, 3555–3567.
- Griffin, R. J., D. Dabdub, and J. H. Seinfeld (2002a), Secondary organic aerosol: 1. Atmospheric chemical mechanism for production of molecular constituents, *J. Geophys. Res.*, 107(D17), 4332, doi:10.1029/2001JD000541.
- Griffin, R. J., D. Dabdub, M. J. Kleeman, M. P. Fraser, G. R. Cass, and J. H. Seinfeld (2002b), Secondary organic aerosol: 3. Urban/regional scale model of size- and composition-resolved aerosols, *J. Geophys. Res.*, 107(D17), 4334, doi:10.1029/2001JD000544.
- Griffin, R. J., K. Nguyen, D. Dabdub, and J. H. Seinfeld (2003), A combined hydrophobic-hydrophilic module for predicting secondary organic aerosol formation, *J. Atmos. Chem.*, *44*, 171–190.
- Griffin, R. J., M. K. Revelle, and D. Dabdub (2004), Modeling the oxidative capacity of the atmosphere of the South Coast Air Basin of California. 1. Ozone formation metrics, *Environ. Sci. Technol.*, 38, 746–752.
- Griffin, R. J., D. Dabdub, and J. H. Seinfeld (2005), Development and initial evaluation of a dynamic species-resolved model for gas-phase chemistry and size-resolved gas/particle partitioning associated with secondary organic aerosol formation, *J. Geophys. Res.*, 110, D05304, doi:10.1029/2004JD005219.
- Harley, R. A., and G. R. Cass (1994), Modeling the concentrations of gasphase toxic organic air pollutants: Direct emissions and atmospheric formation, *Environ. Sci. Technol.*, 28, 88–98.
- Harley, R. A., and G. R. Cass (1995), Modeling the atmospheric concentrations of individual volatile organic compounds, *Atmos. Environ.*, 29, 905–922.
- Harley, R. A., A. G. Russell, G. J. McRae, G. R. Cass, and J. H. Seinfeld (1993), Photochemical modeling of the Southern California Air Quality Study, *Environ. Sci. Technol.*, 27, 378–388.
 Hoffmann, T., J. R. Odum, F. Bowman, D. Collins, D. Klockow, R. C.
- Hoffmann, T., J. R. Odum, F. Bowman, D. Collins, D. Klockow, R. C. Flagan, and J. H. Seinfeld (1997), Formation of organic aerosols from the oxidation of biogenic hydrocarbons, *J. Atmos. Chem.*, 26, 189–222.
- Jang, M. S., N. M. Czoschke, S. Lee, and R. M. Kamens (2002), Heterogeneous atmospheric aerosol production by acid-catalyzed particle-phase reactions, *Science*, 298, 814–817.
- Kalberer, M., et al. (2004), Identification of polymers as major components of atmospheric organic aerosols, Science, 303, 1659–1662.
- Kim, S., S. Shen, C. Sioutas, Y. F. Zhu, and W. C. Hinds (2002), Size distribution and diurnal and seasonal trends of ultrafine particles in source and receptor sites of the Los Angeles Basin, *J. Air Waste Manage. Assoc.*, 52(3), 297–307.
- Kim, Y. P., J. H. Seinfeld, and P. Saxena (1993), Atmospheric gas-aerosol equilibrium I. Thermodynamic model, *Aerosol Sci. Technol.*, 19, 157–181.
- Koo, B., A. S. Ansari, and S. N. Pandis (2003), Integrated approaches to modeling the organic and inorganic atmospheric aerosol components, *Atmos. Environ.*, 37, 4757–4768.
- Lack, D. A., X. X. Tie, N. D. Bofinger, A. N. Wiegand, and S. Madronich (2004), Seasonal variability of secondary organic aerosol: A global modeling study, *J. Geophys. Res.*, 109, D03203, doi:10.1029/2003JD003418.
- Liang, C. K., J. F. Pankow, J. R. Odum, and J. H. Seinfeld (1997), Gas/particle partitioning of semi-volatile organic compounds to model inorganic, organic, and ambient smog aerosols, *Environ. Sci. Technol.*, 32, 3086–3092
- McRae, G. J., and J. H. Seinfeld (1982), Development of a second-generation mathematical model for urban air pollution. 1. Model formulation, Atmos. Environ., 16, 679–696.
- Meng, Z., J. H. Seinfeld, P. Saxena, and Y. P. Kim (1995), Atmospheric gasaerosol equilibrium 4. Thermodynamics of carbonates, *Aerosol Sci. Tech*nol., 23, 131–154.
- Meng, Z., D. Dabdub, and J. H. Seinfeld (1998), Size-resolved and chemically resolved model of atmospheric aerosol dynamics, *J. Geophys. Res.*, 103, 3419–3435.
- Millet, D. B., N. M. Donahue, S. N. Pandis, A. Polidori, C. O. Stanier, B. J. Turpin, and A. H. Goldstein (2005), Atmospheric volatile organic compound measurements during the Pittsburgh Air Quality Study: Results, interpretation, and quantification of primary and secondary contributions, J. Geophys. Res., 110, D07S07, doi:10.1029/2004JD004601.
- Ming, Y., and L. M. Russell (2002), Thermodynamic equilibrium of organic-electrolyte mixtures in aerosol particles, *AIChE J.*, 48, 1331–1348.
- Na, K., A. Á. Sawant, C. Song, and D. R. Cocker III (2004), Primary and secondary carbonaceous species in the atmosphere of western Riverside county, California, Atmos. Environ., 38, 1345–1355.
- Nguyen, K., and D. Dabdub (2001), Two level time marching scheme using splines for solving the advection equation, *Atmos. Environ.*, 35, 1627–1637

- Nguyen, K., and D. Dabdub (2002), Semi-Lagrangian flux scheme for the solution of the aerosol condensation/evaporation equation, *Aerosol Sci. Technol.*, *36*, 407–418.
- Odum, J. R., T. Hoffmann, F. Bowman, D. Collins, R. C. Flagan, and J. H. Seinfeld (1996), Gas/particle partitioning and secondary organic aerosol yields, *Environ. Sci. Technol.*, 30, 2580–2585.
 Odum, J. R., T. P. W. Jungkamp, R. J. Griffin, R. C. Flagan, and J. H.
- Odum, J. R., T. P. W. Jungkamp, R. J. Griffin, R. C. Flagan, and J. H. Seinfeld (1997), The atmospheric aerosol-forming potential of whole gasoline vapor, *Science*, 276, 96–99.
- Pandis, S. N., R. H. Harley, G. R. Cass, and J. H. Seinfeld (1992), Secondary organic aerosol formation and transport, *Atmos. Environ., Part A*, 26, 2269–2282.
- Pankow, J. F. (1994a), An absorption model of gas/particle partitioning of organic compounds in the atmosphere, Atmos. Environ., 28, 185–188.
- Pankow, J. F. (1994b), An absorption model of gas/particle partitioning involved in the formation of secondary organic aerosol, *Atmos. Environ.*, 28, 189–193.
- Pun, B. K., R. J. Griffin, C. Seigneur, and J. H. Seinfeld (2002), Secondary organic aerosol: 2. Thermodynamic model for gas/particle partitioning of molecular constituents, *J. Geophys. Res.*, 107(D17), 4333, doi:10.1029/ 2001JD000542.
- Pun, B. K., S. Y. Wu, C. Seigneur, J. H. Seinfeld, R. J. Griffin, and S. N. Pandis (2003), Uncertainties in modeling secondary organic aerosols: Three-dimensional modeling studies in Nashville/western Tennessee, *Environ. Sci. Technol.*, 37(16), 3647–3661.
- Sardar, S. B., P. M. Fine, and C. Sioutas (2005), Seasonal and spatial variability of the size-resolved chemical composition of particulate matter (PM₁₀) in the Los Angeles Basin, *J. Geophys. Res.*, 110, D07S08, doi:10.1029/2004JD004627.
- Saxena, P., and L. M. Hildemann (1996), Water-soluble organics in atmospheric particles: A critical review of the literature and application of thermodynamics to identify candidate compounds, *J. Atmos. Chem.*, 24, 57–109.
- Saxena, P., L. M. Hildemann, P. H. McMurry, and J. H. Seinfeld (1995), Organics alter hygroscopic behavior of atmospheric particles., *J. Geo*phys. Res., 100, 18,755–18,770.
- Schell, B., I. J. Ackermann, H. Hass, F. S. Binkowski, and A. Ebel (2001), Modeling the formation of secondary organic aerosol within a comprehensive air quality model system, *J. Geophys. Res.*, 106, 28,275–28,293.
- Seinfeld, J. H. (2004), Air pollution: A half century of progress, AIChE J., 50, 1096–1108.

- Seinfeld, J. H., and S. N. Pandis (1998), Atmospheric Chemistry and Physics, Wiley-Interscience, Hoboken, N. J.
- Sheehan, P. E., and F. M. Bowman (2001), Estimated effects of temperature on secondary organic aerosol concentrations, *Environ. Sci. Technol.*, 35, 1806–1817.
- Stockwell, W. R., F. Kirchner, M. Kuhn, and S. Seefeld (1997), A new mechanism for regional atmospheric chemistry modeling, *J. Geophys. Res.*, 102, 25,847–25,879.
- Strader, R., F. Lurmann, and S. N. Pandis (1999), Evaluation of secondary organic aerosol formation in winter, *Atmos. Environ.*, 33, 4849–4863.
- Takekawa, H., H. Minoura, and S. Yamazaki (2003), Temperature dependence of secondary organic aerosol formation by photo-oxidation of hydrocarbons, *Atmos. Environ.*, 37, 3413–3424.
- Tsigaridis, K., and M. Kanakidou (2003), Global modelling of secondary organic aerosol in the troposphere, *Atmos. Chem. Phys.*, *3*, 1849–1869.
- Turpin, B. J., and J. J. Huntzicker (1991), Secondary formation of organic aerosol in the Los Angeles Basin: A descriptive analysis of organic and elemental carbon concentrations, Atmos. Environ., Part A, 25, 207–215.
- Turpin, B. J., and J. J. Huntzicker (1995), Identification of secondary organic aerosol episodes and quantitation of primary and secondary organic aerosol concentrations during SCAQS, Atmos. Environ., 29, 3527–3544.
- Turpin, B. J., S. Pradeep, and E. Andrews (2000), Measuring and simulating particulate organics in the atmosphere: Problems and prospects, Atmos. Environ., 34, 2983–3013.
- Xiong, J. Q., M. H. Zhong, C. P. Fang, L. C. Chen, and M. Lippmann (1998), Influence of organic films on the hygroscopicity of ultrafine sulfuric acid aerosol, *Environ. Sci. Technol.*, 32, 3536–3541.
- Yu, J., D. R. Cocker III, R. J. Griffin, R. C. Flagan, and J. H. Seinfeld (1999), Gas-phase ozone oxidation of monoterpenes: Gaseous and particulate products, *J. Atmos. Chem.*, 34, 207–258.
- D. Dabdub and S. Vutukuru, Department of Mechanical and Aerospace Engineering, University of California, Irvine, CA 92697, USA. (ddabdub@uci.edu; satish@uci.edu)
- R. J. Griffin, Institute for the Study of Earth, Oceans and Space, University of New Hampshire, Durham, NH 03824, USA. (rob.griffin@unh.edu)